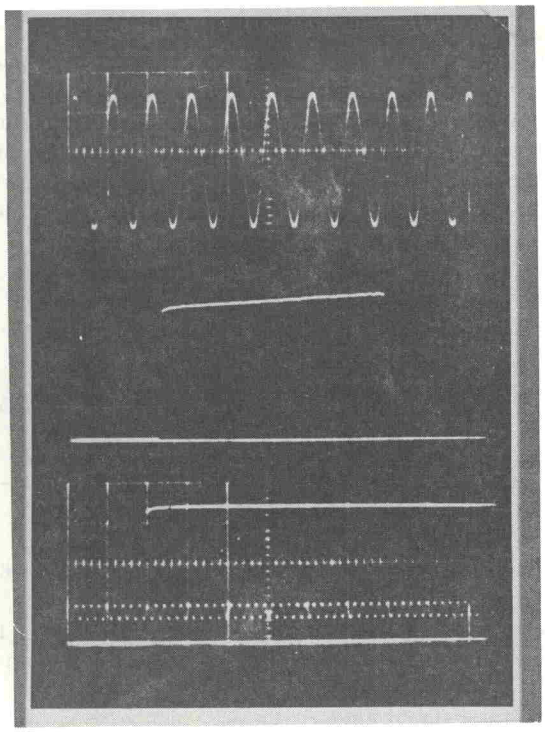

FIG. 2. Current amplitude vs time for a typical oscilloscope record is shown in the center trace. Time increases from left to right. The upper and lower traces are amplitude and timing calibration records taken immediately following the experiment. About 450 nsec prior to impact, the trace is triggered. The impact is indicated by the sharp jump in current followed by a gradual increase in current to shock-wave transit time which is indicated by a sharp decrease in signal amplitude 1.11 μsec after impact. The current amplitude is 0.67 A at a strain of 2.8×10^{-2}.

solute accuracy of the current–vs–time-pulse measurements. The considerable care and special calibrations employed to give an over-all maximum experimental error of between $\frac{1}{2}$ and 1% have been previously described in the technique article.[25]

A typical current-vs-time record is shown in Fig. 2. The response shows a jump to a first steady current value followed by a slight linear increase in current up to wave transit time. Note that the transit time of the shock wave through the sample is marked by a sharp discontinuity in current. Features of this current pulse will be interpreted in terms of the electrostatic model developed in Sec. IV.

IV. PIEZOELECTRIC-PULSE ANALYSIS

The experiments provide measures of the particle velocities imparted to the samples, the transit time of the elastic shock waves through known thicknesses, and the time-resolved amplitude of the short-circuited current. In this section the relationships among these experimental measurements and the corresponding elastic, piezoelectric, and dielectric properties will be established. The conservation of mass and momentum are used to compute the stress and linear strain, while an electrostatic analysis is used to determine piezoelectric polarization from the current-pulse measurement. Finally, a small correction is applied to the electrostatic analysis to include the effect of electromechanical coupling.

A. Characterization of Elastic Shock Waves

Shock waves in solids have been extensively utilized to determine the very high-pressure equation of state.[27] At very high pressure the solid is typically considered to react as a fluid since the pressure greatly exceeds the shear strength of the solid.[28] At lower pressures the solid may be treated as an elastic-plastic solid.[29] In the present case the solid has an unusually large shear strength, and stress amplitudes are limited to values less than that required to exceed the shear strength. In spite of the different material properties, the characterization of the shock compression may be accomplished with the conservation of momentum and mass across the shock front.

Consider a steady nondissipative elastic shock wave moving into an unstressed medium at rest. Behind the shock front the material moves with a particle velocity u and is stressed to a longitudinal stress σ. The conservation of momentum across the shock front may be expressed as

$$\sigma_1 = \rho_0 U u \,, \tag{11}$$

where σ_1 is the component of compressive stress in the propagation direction, ρ_0 the unstressed density, u the particle velocity imparted by the shock front, and U the shock-wave velocity. [In the low-strain limit, $U=(c_{11}/\rho_0)^{1/2}$.] From the conservation of mass across the shock front, the uniaxial compression γ can be written as

$$\gamma = u/U \,. \tag{12}$$

The experiments provide a measure of both U and u; therefore, sufficient data are obtained to compute both the linear uniaxial compression and the stress achieved in each experiment.

The material-strain measure which includes quadratic differential elements, Eq. (2), can be computed from each linear compression point through the coordinate transformation which was formally developed by Fowles.[15] Thus, in uniaxial compression,

$$\eta_1 = \gamma(\tfrac{1}{2}\gamma - 1) \,. \tag{13}$$

Similarly, the thermodynamic tension, which is used to compute the high-order constants, Eq. (3), can be computed from the stress by the transformation

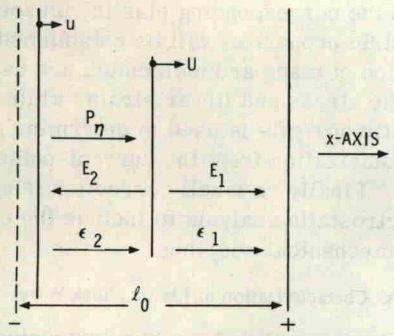

FIG. 3. Electrostatic model used to interpret the current-vs-time records is depicted by a section through the uniaxial sample at a typical time. The shock front, moving from left to right at a velocity U, divides the sample into two characteristic regions. Behind the front, the sample is strained to a constant value of piezoelectric polarization P_η. To accommodate the electric short circuit between the two electrodes, electric fields E_1 and E_2 are developed in both the strained and unstrained regions. The strained permittivity ϵ_2 and unstrained permittivity ϵ_1 are characteristic of the two regions. The left electrode moves with a velocity u which acts to cause a small decrease in thickness in time.

$$t_1 = \sigma_1(\gamma - 1)^{-1}. \tag{14}$$

The shock-induced temperature rise due to adiabatic compression can be readily computed. At the maximum compression utilized in these experiments, the temperature rise is 10 °C. This increase in temperature will cause fractional changes in the elastic stiffness c_{11}, the piezoelectric stress constant e_{11}, and the permittivity ϵ_1 of 4.9×10^{-4}, 1.6×10^{-3}, and 2.8×10^{-4}, respectively.[30] These changes are negligible in the present experiments; hence, temperature effects will be neglected.

B. Electrostatic Configuration

The propagation of an elastic shock wave through a piezoelectric solid with short-circuited electrodes will be described in terms of the electrostatic configuration shown in Fig. 3. A section through a one-dimensional region of the disk shows the shock front at a typical time before traversing the thickness of the disk. In moving from left to right, the shock front divides the disk into two characteristic electrostatic regions. In the region behind the shock front the sample is strained to a constant value of piezoelectric polarization P_η. To accommodate the short-circuited condition between the electrodes, time-dependent electric fields $E(t)$ are developed with polarities as shown. The left face of the disk moves with particle velocity u. The polarization, strain, and electric fields are collinear along the x axis of the disk.

The shock wave moves with a speed slow compared to the speed of an electromagnetic disturbance; hence, the analysis utilizes electrostatic solutions and neglects electromechanical coupling effects. Since quartz has a small value for electromechanical coupling, the weak-coupling solution provides an excellent approximation to the present experiments and the electromechanical coupling effects can be treated as a small perturbation to the electrostatic solution.

C. Electrostatic Analysis

It is convenient to define the electric displacement D as

$$D = P_\eta + \epsilon E, \tag{15}$$

where P_η is the piezoelectric polarization and ϵ is the permittivity. The analysis will obtain a solution for the displacement current i,

$$i = A\frac{dD}{dt}, \tag{16}$$

where A is the area of the collecting electrode. If there is no free charge in the disk, i.e., the conductivity[31] equals zero, $\nabla\cdot\vec{D}=0$; hence, for the one-dimensional case,

$$\frac{\partial D}{\partial x} = 0. \tag{17}$$

The electrical short circuit imposes the following condition between the electrodes:

$$\int_{\text{thickness}} E(x)\,dx = 0. \tag{18}$$

The basic conditions expressed in Eqs. (15)–(18) can be readily applied to the particular configuration used in these experiments. The short-circuit condition of Eq. (18) leads to

$$E_1(t)l_1(t) + E_2(t)l_2(t) = 0, \tag{19}$$

where l_1 and l_2 are the time-dependent thicknesses of the unstressed and stressed regions. From Eq. (17) it follows that

$$P_\eta + \epsilon_2 E_2 = \epsilon_1 E_1. \tag{20}$$

Equations (19) and (20) thus lead to the result that

$$D = \epsilon_1 E_1 = P_\eta[1 + \alpha l_1(t)/l_2(t)]^{-1}, \tag{21}$$

where α is the ratio of the strained-to-unstrained permittivity ϵ_2/ϵ_1; $l_1 = l_0 - Ut$; and $l_2 = (U-u)t$. The displacement current is then

$$\frac{i(t)t_0}{P_\eta A} = \frac{\alpha(1-u/U)}{[(1-u/U)(t/t_0) + \alpha(1-t/t_0)]^2}, \quad 0 < t < t_0 \tag{22}$$

where $t_0 = l_0U^{-1}$, the shock-wave transit time.

In the normalized form shown in Eq. (22), the current is close to a unit step function. This is apparent when the maximum value of $u/U = 0.04$ and the maximum value of $\alpha = 1.02$ are substituted into the equation. The form of this solution is in